Eur. Phys. J. A **24**, 57–62 (2005)
DOI 10.1140/epja/i2004-10124-7

THE EUROPEAN PHYSICAL JOURNAL A

Prolate structures in ^{189}Po and ^{185}Pb

K. Van de Vel[1,6,a], A.N. Andreyev[2,7,b], D. Ackermann[3,8], H.J. Boardman[2], P. Cagarda[3], J. Gerl[3], F.P. Heßberger[3], S. Hofmann[3,9], M. Huyse[1], D. Karlgren[1,4], I. Kojouharov[3], M. Leino[5], B. Lommel[3], G. Münzenberg[3,8], C. Moore[2], R.D. Page[2], S. Saro[3], P. Van Duppen[1], and R. Wyss[4]

[1] Instituut voor Kern- en Stralingsfysica, University of Leuven, Celestijnenlaan 200D, 3001 Leuven, Belgium
[2] Oliver Lodge Laboratory, University of Liverpool, Liverpool L69 7ZE, UK
[3] Gesellschaft für Schwerionenforschung, Planckstrasse 1, 64291 Darmstadt, Germany
[4] Department of Physics, Royal Institute of Technology, 104 05 Stockholm, Sweden
[5] Department of Physics, University of Jyväskylä, 40014 Jyväskylä, Finland
[6] Flemish Institute for Technological Research (VITO), Boeretang 200, 2400 Mol, Belgium
[7] TRIUMF, 4004 Wesbrook Mall, Vancouver B.C., Canada
[8] Johannes Gutenberg Universität Mainz, 55099 Mainz, Germany
[9] Physikalisches Institut, J.W. Goethe-Universität, 60054 Frankfurt, Germany

Received: 15 April 2004 / Revised version: 7 January 2005 /
Published online: 25 January 2005 –
Communicated by J. Äystö

Abstract. The $3/2^-$ isomer in ^{185}Pb and states above it have been populated in the α-decay of ^{189}Po. The observed α-decay strengths to and the electromagnetic decay properties of the excited states in ^{185}Pb have been combined with Potential Energy Surface and Particle-Plus-Rotor calculations to propose configuration assignments. It is suggested that the α-decaying isomer of ^{189}Po is of prolate origin and that the prolate configuration becomes very low in energy in ^{185}Pb.

PACS. 23.20.Lv γ transitions and level energies – 23.20.Nx Internal conversion and extranuclear effects – 23.60.+e α decay – 27.70.+q $150 \leq A \leq 189$

1 Introduction

Shape coexistence in the neutron-deficient polonium isotopes is a well-established phenomenon as discussed in [1–7] and references therein. Extensive studies of the level structure and the α-decay properties of the long chain of even-mass Po isotopes show that the nuclei down to ^{198}Po can be considered as near spherical anharmonic vibrators [4,7,8]. With decreasing neutron number an oblate deformed configuration intrudes into the low-energy part of the excitation spectrum. For example, based on in-beam and α-decay data the oblate structure is found to comprise $\sim 70\%$ and 40% of the ground-state configuration in ^{192}Po and ^{194}Po, respectively [4,7]. A recent in-beam study of ^{190}Po provided evidence that the prolate deformed configuration becomes yrast above spin 4 $\hbar$ [9].

A similar picture of shape coexistence is observed in the odd-mass Po isotopes. Down to ^{197}Po the lowest states can be interpreted as arising from the weak coupling of an odd neutron to the nearly spherical core of the neighbouring even-mass isotope. A gradual transition to a strongly coupled band structure in ^{191,193,195}Po hints at the onset of oblate deformation for the $13/2^+$ isomer of ^{191}Po [4, 10]. The experimental observations are in agreement with Potential Energy Surface (PES) calculations as illustrated in [3,10,11]. One of the important conclusions of these calculations is that the prolate configuration becomes lowest in energy in the mid-shell nuclei ^{188}Po [11] and in ^{189}Po. Unfortunately, due to low-production cross-sections (at most a few tens of nanobarns) in-beam studies of ^{188,189}Po are currently not possible. However, as shown in our extensive studies, α-decay is a powerful tool to investigate shape coexistence in the lead region, quite often providing unique information on the excitation energy of the coexisting configurations in the daughter nucleus and on the structure of both the parent and daughter nuclei [6]. For example, in our recent work evidence for the onset of prolate deformation in ^{188}Po was discussed based on the fine structure observed in the α-decay pattern [11]. In this work we discuss the fine structure observed in the α-decay of ^{189}Po.

The isotope ^{189}Po was identified by Andreyev *et al.* [12], who observed three α-decay transitions with energies and corresponding intensities of 7540(20) keV

[a] e-mail: karen.vandevel@vito.be
[b] e-mail: andreyev@triumf.ca

(11(5)%), 7264(15) keV (76(5)%) and 7316(15) keV (13(5)%). These decays were assigned to one isomer of ^{189}Po with a half-life of 5(1) ms. Neither spin and parity nor configuration assignments could be made to the α-decaying state in ^{189}Po and to the excited states in the daughter ^{185}Pb mainly due to the poor knowledge of the decay scheme of ^{185}Pb. Recently in a laser spectroscopy experiment spins and parities of $13/2^+$ and $3/2^-$ were assigned to two α-decaying states of ^{185}Pb and their decay properties were studied in detail [13].

The structure of the present paper is as follows: after a brief discussion of the experimental set-up (sect. 2), we present the improved experimental data (statistics increased by a factor of 3 compared with the data discussed in [12]) together with the main ideas applied in the data analysis of ^{189}Po (sect. 3). The main emphasis is put on the results of the potential energy surface calculations and particle-rotor calculations, discussed in details in sect. 4, which together with the improved experimental data allowed us to shed more light on the shape coexistence in both ^{189}Po and ^{185}Pb.

2 Experimental set-up

The experiment was performed at the velocity filter SHIP at GSI, Darmstadt, using the same detection set-up as in the earlier study [12] in which the complete-fusion reaction ^{52}Cr + ^{142}Nd $\rightarrow$ ^{194}Po* was employed. We therefore only summarize the experimental details and refer to [12] for a complete overview of the experimental procedure. The nuclei were produced in the ^{142}Nd (^{52}Cr, 5n)^{189}Po and ^{142}Nd (^{50}Cr, 3n)^{189}Po reactions with cross-sections of 20 nb and 30 nb, respectively. The ^{142}Nd targets (isotopic enrichment of 99.8%) with a thickness of 290 μg/cm^2 were evaporated as $^{142}Nd_2F_3$ material onto carbon layers of 50 μg/cm^2 thickness and covered with a 10 μg/cm^2 layer of carbon. The Cr beams were provided by the heavy-ion accelerator UNILAC with a beam energy of 5.27 AMeV (in front of the target) for ^{52}Cr optimized for the 5n evaporation channel, the majority of the data obtained for ^{189}Po come from this reaction. In the ^{50}Cr + ^{142}Nd reaction the beam energy of 5.04 AMeV was optimized for the production of ^{188}Po and it adds only about 15% to the statistics for ^{189}Po. The Cr beams had a pulsed structure with 5 ms on/15 ms off and a typical intensity of 200 pnA. The recoiling nuclei were separated from the beam particles by the velocity filter SHIP [14,15] and were implanted into a (80 $\times$ 35) mm^2 300 μm thick Position-Sensitive Silicon strip Detector (PSSD) at the focal plane of SHIP. In front of the PSSD six silicon detectors of the same shape were arranged in an open-box geometry. These were used to detect conversion electrons within 5 μs from the detection of an α-particle. We note that α-particles escaping from the PSSD can also give a signal in these detectors. Coincidences between α-particles and γ-rays were measured (within a time interval of 5 μs) with a fourfold segmented Clover germanium detector mounted directly behind the PSSD.

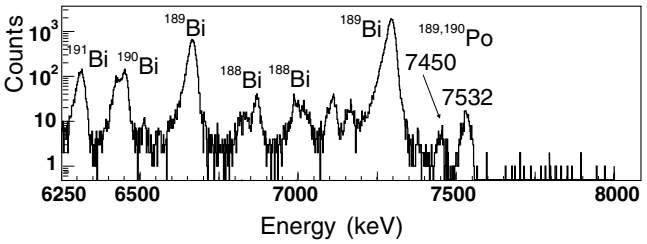

Fig. 1. Energy spectrum of α-particles following the implantation of a recoil in the PSSD within a time interval of 15 ms for the ^{50,52}Cr + ^{142}Nd reactions.

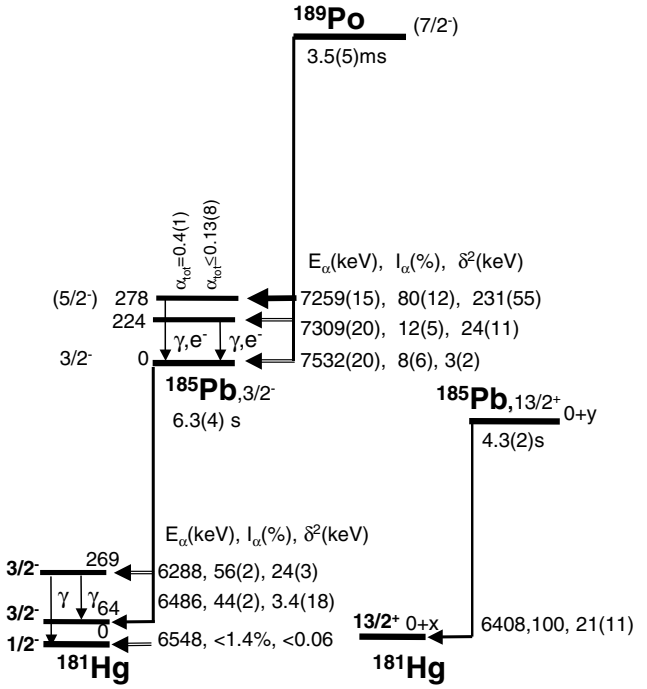

Fig. 2. Decay chain of ^{189}Po-^{185}Pb-^{181}Hg. The data for the decay of ^{185}Pb are taken from [13].

3 Experimental results

The data analysis of the present experiment is similar to the one described in [12] and therefore only some representative features and spectra are mentioned here. From the present experiment with the ^{52}Cr beam the energy spectrum of α-particles following the implantation of a recoil in the PSSD within a time interval of 15 ms is shown in fig. 1. As the beam energy is the same as used in our first experiment, this spectrum is very similar to fig. 1a of [12]. Also α-γ and α-e$^-$ coincidence spectra were obtained, which are very similar to those of fig. 1b, c of [12], respectively, and therefore we do not show them here. In all these spectra we obtained an increase in statistics by a factor of three compared with the data discussed in [12]. Based on the combined statistics from the two experiments, improved values for the half-life, energies and intensities of the fine structure α lines of ^{189}Po and for the conversion coefficients of the transitions in the daughter ^{185}Pb were obtained. The resulting decay scheme is shown in fig. 2 and will be discussed in detail below.

We confirmed the observation of the α(7259(15) keV)-γ(278(2) keV) and α(7309(20) keV)-γ(224(2) keV) decays of ^{189}Po from ref. [12]. Based on the sum $Q_{\alpha,\mathrm{sum}} = Q_\alpha + E_\gamma$ value for these decays a direct crossover transition of 7532 keV could be expected and fig. 1 indeed shows a peak at 7532(20) keV. However, to determine the intensity of this transition one needs to correct for the contribution of ^{190}Po having an α-decay energy of 7533 keV and a half-life of 2.45(5) ms [5]. ^{190}Po is produced in the same reaction in the 4n channel. The separation of ^{189,190}Po was performed using recoil-α_1-α_2 correlations as discussed below. Since the 7259 keV-278 keV and 7309 keV-224 keV coincident pairs have the same $Q_{\alpha,\mathrm{sum}}$ value and since they show a similar decay time, they were attributed to the decay of the same isomer in ^{189}Po with a half-life of 3.5(5) ms, in agreement with the previously reported value of 5(1) ms [12].

The excited states at 278 keV and 224 keV in ^{185}Pb also decay via conversion electron emission, the peak at 7450(15) keV in fig. 1 corresponds to events for which the total electron energy ($E_{e^-} = E_\gamma - BE$ where $BE = 88$ keV is the binding energy of a K-shell conversion electron in Pb) is summed up in the PSSD with the fine-structure α-particle energy.

By using the method from [12] and by comparing the α-electron and α-γ spectra (see fig. 1 of [12]) we deduced a value of $\alpha_{\mathrm{tot}} = 0.4(1)$ for the total conversion coefficient of the 278 keV transition. This value is in agreement with $\alpha_{\mathrm{tot}} = 0.61(15)$ deduced in [12]. The quoted error of the conversion coefficient takes into account both the statistical and the systematic uncertainties. The latter uncertainty is determined by the uncertainties in the conversion electron efficiency determination of the backward detectors used for conversion electron measurements, by α-electron energy summing in the PSSD and by the uncertainty for the efficiency measurements for the γ- and X-rays in the Clover Ge detector (discussed extensively in refs. [5,12]).

For the first time an upper limit of $\alpha_{\mathrm{tot}} = 0.13(8)$ was deduced for the total conversion coefficient of the 224 keV decay. The comparison of the conversion coefficient for the 278 keV transition with theoretical values of 0.035 ($E1$), 0.147 ($E2$), 0.85 ($E3$) and 0.547 ($M1$) points to a pure $M1$, or mixed $E0$-$M1$-$E2$ or mixed $E1$-$E3$ character. The latter is excluded by the short half-life of the transition.

A half-life for the 278 keV level in ^{185}Pb was obtained on the basis of the distribution of the time difference between the α-particle and the subsequent γ-ray or conversion electron. Figure 3 compares the α-γ time differences for a) the 7259 keV-278 keV decays of ^{189}Po and b) for the known 34(4) ns 184 keV isomer in ^{188}Tl populated in the α-decay of ^{192}Bi [16]. The ^{192}Bi nuclei were produced in the ^{52}Cr + ^{142}Nd reaction at a beam energy of 4.33 AMeV in front of the target. Note that spectrum 3b) practically does not have any random background above channel 3400. The comparison of the two spectra clearly shows that the 278 keV transition has a longer half-life than the 184 keV decay in ^{186}Tl, a half-life of 200^{+100}_{-50} ns was deduced. The upper limit of $\alpha_{\mathrm{tot}} = 0.13(8)$ for the

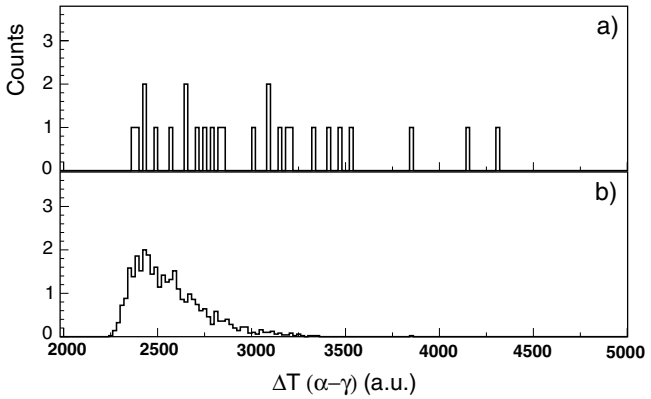

Fig. 3. Time difference between an α-particle and a γ-ray for a) the 7259-278 keV fine-structure α-decay of ^{189}Po and b) the 34(4) ns 184 keV transition in ^{188}Tl.

conversion coefficient of the 224 keV transition points at a $\Delta L \leq 2$ transition. Due to low statistics the timing analysis could not be done for the 224 keV state.

In order to determine which isomer ($13/2^+$ or $3/2^-$) of ^{185}Pb is populated in the α-decay, recoil-α_1(^{189}Po)-α_2(^{185}Pb) correlations were carried out. The decay scheme of ^{185}Pb is shown in the bottom part of fig. 2. The recoil-α_1 and α_1-α_2 correlation times were set to 15 ms and 12 s, respectively. We note that the relative positions of the isomers in ^{185}Pb and ^{181}Hg are unknown. Correlations were found for the α(7259 keV)-γ(278 keV), α(7309 keV)-γ(224 keV) and α(7259 keV)-electron decays of ^{189}Po with the alpha decay of the $3/2^-$ isomer of ^{185}Pb, including one correlation chain of the type recoil-[α_1(7249 keV)-γ(278 keV)]-[α_2(6269 keV)-γ(269 keV)] with ΔT(recoil-α_1) = 2.28 ms and $\Delta T(\alpha_1$-$\alpha_2) = 8.5$ s. A branching ratio of 34(25)% was deduced for the α-decay of the $3/2^-$ state of ^{185}Pb. No correlations were found with the α-decay of the $13/2^+$ isomer of ^{185}Pb.

The contribution of ^{189,190}Po to the 7532 keV peak in fig. 1 was estimated from the recoil-α_1(^{189,190}Po)-α_2(^{185,186}Pb) correlation analysis (see details in ref. [17]). The ^{189}Po contribution was found to be 27(20)% using the α-decay branching ratio of 38(9)% for ^{186}Pb [17]. This results in a branching ratio for the $3/2^-$ decay of ^{185}Pb that is in agreement within the error with the aforementioned 34(25)%. The intensities and reduced α-decay widths (δ^2) of the fine-structure α lines and the crossover 7532 keV decay of ^{189}Po are indicated in fig. 2. The reduced α-decay width measures the α-decay transition probability after the energy dependence of the tunnelling through the Coulomb barrier is taken away. The δ^2 values were calculated using the formalism of Rasmussen [18] for $\Delta L = 0$ transitions.

4 Discussion

In order to interpret the decay scheme of ^{189}Po we combine various experimental and theoretical results. We first summarize the main characteristics of the α-decay of ^{189}Po

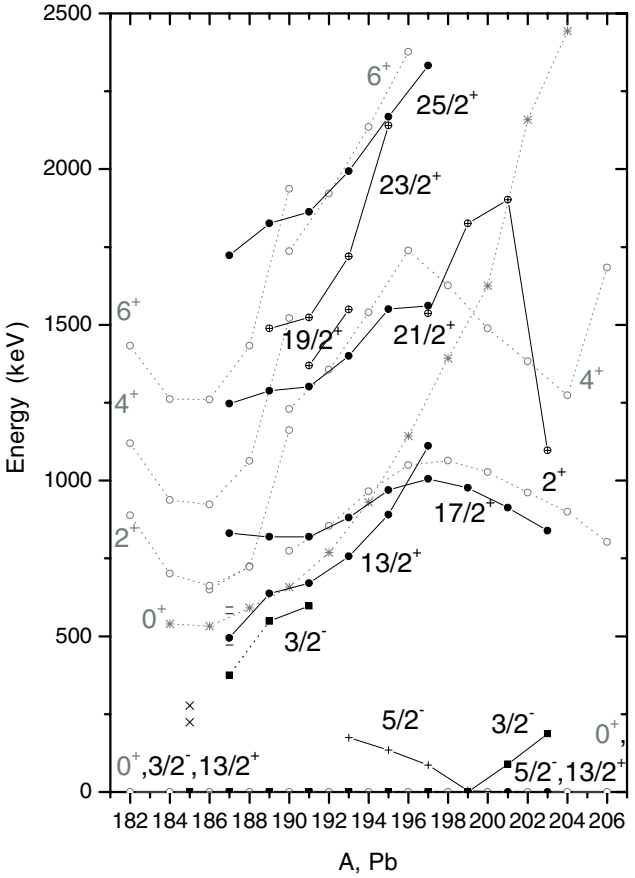

Fig. 4. Low-energy level systematics for selected configurations in the light lead isotopes. The yrast 0^+–6^+ states in the even-even nuclei are shown with empty circles, the 0_2^+ states by crosses. For the odd-mass nuclei the positive-parity states are indicated with filled and crossed circles, in ^{187}Pb positive-parity states are indicated with horizontal bars. The negative-parity states are shown with filled squares ($3/2^-$ states), plus signs ($5/2^-$ states) and crosses (in ^{185}Pb). In the odd-mass nuclei for $A \leq 199$ they are shown relative to the lowest $3/2^-$, $13/2^+$ states for the negative-, positive-parity states, respectively. The $5/2^-$ configuration is the lowest for $A > 199$.

studied in the present study. We then combine these findings with the results of a laser spectroscopy and α-decay study of ^{185}Pb (discussed in [13]) . The final assignments to the states in ^{189}Po and ^{185}Pb can be made with the help of Potential Energy Surface (PES) and Particle-Plus-Rotor (PPR) calculations.

Firstly the excited states identified in ^{185}Pb are included in the energy systematics of the excited states in the odd-mass Pb isotopes. Figure 4 shows the excited states above the $13/2^+$ and $3/2^-$ states in $^{185-203}$Pb, they have been identified in in-beam studies and in β^+/EC- and α-decay studies. In the odd-mass nuclei for $A \leq 199$ the excited negative- and positive-parity states are shown relative to the lowest $3/2^-$ and $13/2^+$ states, respectively. The $5/2^-$ configuration is the lowest for $A > 199$. The lowest positive-parity excited states in $^{187-193}$Pb and the lowest negative-parity excited states in $^{189-191}$Pb have been associated to the oblate configuration due to the coupling of the $i_{13/2}$ and $p_{3/2}$ valence neutrons, respectively, to the oblate even-even lead core [10,11]. Figure 4 shows that the excited states above the $3/2^-$ isomer in ^{185}Pb lie at a very low excitation energy compared to the first-excited state identified in the heavier odd-mass Pb isotopes and to the 2^+ states in the even-mass Pb isotopes. Based on the $3/2^-$ assignment to the lowest state of the low-spin isomer of ^{185}Pb and the measured conversion coefficient of the 278 keV transition, the pure $M1$ or mixed $E0$-$M1$-$E2$ character of the 278 keV transition in ^{185}Pb gives a possible spin/parity assignment of $1/2^-$-$5/2^-$ or $3/2^-$, respectively, for the state at 278 keV. The 200^{+100}_{-50} ns half-life of the 278 keV state in ^{185}Pb yields a decay strength of 10^{-2} W.u. or 2×10^{-6} W.u. by assuming an $E2$ or $M1$ transition, respectively. For the 224 keV state in ^{185}Pb, the upper limit on the conversion coefficient of the 224 keV transition restricts the spin of the 224 keV state to the 1/2–7/2 range.

The reduced α-decay width for the 7532 keV decay to the $3/2^-$ isomer in ^{185}Pb is very small (3(2) keV, see fig. 2). On the other hand, the 7259 keV decay of ^{189}Po to the 278 keV state in ^{185}Pb has a rather large reduced width, being only slightly lower than the mean value of the neighbouring even-even ^{188,190}Po nuclei [11]. The latter fact is most probably explained by the odd-particle blocking in an odd-A nucleus which gives a reduction in the α-particle formation probability. The ratio $\delta^2(7259\text{ keV})/\delta^2(7532\text{ keV}) = 77$. These experimental observations are very important as they indicate a different structure for the 278 keV state and the $3/2^-$ state in ^{185}Pb, on the one hand, and a very similar structure for the α-decaying isomer of ^{189}Po and for the 278 keV state in the daughter ^{185}Pb, on the other. The present data do not allow to assign unambiguously a configuration to the 224 keV state due to the large error on the reduced width of the feeding α-decay.

The character of the $3/2^-$ isomer in ^{185}Pb was investigated in a laser spectroscopy measurement [13] which showed that there is no major change in the $3/2^-$ configuration for ^{185}Pb compared with the heavier Pb isotopes. The $3/2^-$ isomer in ^{185}Pb is of pure single-particle character, the spherical configuration remains lowest in energy owing to the spherical $Z = 82$ shell gap. The evaluation of the decay properties of the $3/2^-$ state also confirms its single-particle character, originating from the weak coupling of the odd $3p_{3/2}$ neutron to the even-even spherical core [13].

The large difference in the α-decay reduced width and the retarded decay of the 278 keV state to the $3/2^-$ state in ^{185}Pb suggest a different character for both states, indicating a deformed configuration for the excited state as found in the heavier odd- and even-mass Pb nuclei. However, fig. 4 suggested a different configuration for the very low-energy excited states in ^{185}Pb compared to in the heavier odd-mass Pb nuclei.

Potential Energy Surface (PES) and Particle-Plus-Rotor (PPR) calculations were performed in order to shed further light on the configuration of the states observed.

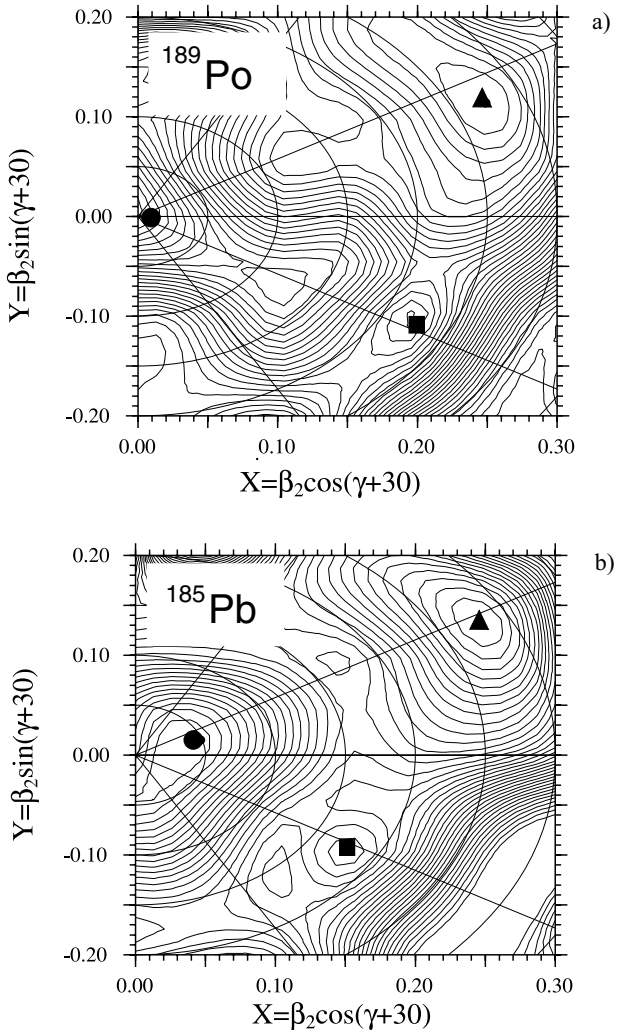

Fig. 5. Potential energy surfaces for (a) ^{189}Po and (b) ^{185}Pb. Spherical, oblate and prolate minima are indicated with circles, squares and triangles, respectively. The energy separation between the contour lines is 50 keV.

The PES calculations performed are identical to the ones described in refs. [3,10,19], ref. [10] is dedicated to a similar decay study for ^{191}Po to ^{187}Pb and also gives a detailed description of the PPR calculations performed in this work. The potential energy surfaces for negative-parity states in ^{189}Po and in ^{185}Pb are shown in fig. 5. In ^{189}Po a prolate deformed minimum at $|\beta_2| = 0.27$ (shown by triangle) is predicted to be lowest in energy, which is a new feature compared with the heavier odd-mass Po isotopes [6,10]. In the daughter ^{185}Pb a spherical minimum coexists with a low-lying prolate minimum at $|\beta_2| = 0.27$ at an excitation energy of only 140 keV. The oblate minimum lies 742 keV above the spherical one. We note that similar minima are predicted for the positive-parity states in ^{189}Po and ^{185}Pb.

Based on the PES calculations and the energy level systematics of the lead isotopes we exclude the oblate configuration assignment to the 224 keV and 278 keV states in ^{185}Pb as they lie lower in energy than expected from an extrapolation of the oblate $3/2^-$ and $13/2^+$ states (from the coupling of the $p_{3/2}$ and $i_{13/2}$ valence neutrons, respectively, to the oblate even-even lead core) observed in the heavier Pb nuclei [10,11]. Also the PES calculations predict that the oblate configuration goes up in energy when moving to more neutron-deficient nuclei and that it has a rather high excitation energy in ^{185}Pb as mentioned above. On the other hand, the prolate configuration comes very low in energy in ^{185}Pb and we therefore propose a prolate configuration for the 278 keV state in ^{185}Pb. Particle Plus Rotor (PPR) calculations carried out in the prolate minimum of the PES of ^{185}Pb give a $5/2^-[512]$ Nilsson state lowest in energy. This spin assignment is in agreement with the $M1$ multipolarity of the 278 keV transition.

As mentioned above the fast decay between the α-decaying state in ^{189}Po and the 278 keV state in ^{185}Pb suggests a similar configuration for both states. A negative parity is adopted for ^{189}Po as a parity change would give rise to a retardation of the 7259 keV α-decay. The PPR calculations give a $7/2^-[514]$ configuration for the negative-parity prolate minimum in ^{189}Po. The main contribution to the prolate $7/2^-[514]$ (α-decaying isomer in ^{189}Po) and prolate $5/2^-[512]$ (excited state at 278 keV in ^{185}Pb) Nilsson states at large prolate configuration $\beta_2 \sim 0.3$ stems from the $f_{7/2}$ and $h_{9/2}$ neutron orbitals.

Finally we would like to comment on two peculiarities observed in the alpha decay of ^{189}Po which can be reconciled with the interpretation given above to the states in ^{189}Po and ^{185}Pb connected by the alpha decay. Firstly only one α-decaying isomer has been observed for ^{189}Po in contrast to the heavier odd-mass isotopes $^{191-201}$Po which have two α-decaying states, see [6,10] and references therein. This observation can be explained by the configuration assignment to ^{189}Po proposed above. The PPR calculations for the positive-parity prolate minimum in ^{189}Po associate it with a prolate deformed $9/2^+[624]$ configuration and give an excitation energy of ~ 100 keV above the prolate $7/2^-[514]$ state. Prompt $E1$ decay from the $9/2^+$ state to the $7/2^-$ state can readily explain the presence of only one α-decaying state. Secondly the decay of a strongly deformed prolate state in ^{189}Po to the spherical $3/2^-$ state in ^{185}Pb can also explain the deviation in the alpha-decay energy of ^{189}Po from the Q_α systematics of the heavier nuclei. The Q_α value of the α-decay of ^{189}Po is about 200 keV lower than the value expected from an extrapolation from the heavier masses as commented on in ref. [6]. As the $3/2^-$ configuration in ^{185}Pb is similar to that of the heavier isotopes, the deviation may arise from the change in the nature of the α-decaying state in ^{189}Po to a strongly deformed prolate state.

5 Conclusions

The fine structure in the α-decay of ^{189}Po has been studied in detail and the states populated in ^{185}Pb have been further characterized. While the $3/2^-$ isomer of ^{185}Pb is of a spherical single-particle configuration, the low-lying 278 keV state above the $3/2^-$ isomer

was associated with a prolate structure on the basis of the α-decay characteristics, the decay properties and PES + PPR calculations. The disappearance of isomerism in ^{189}Po and the deviation from the Q_α systematics are explained by the intruding prolate configuration to become the ground state in ^{189}Po.

We thank the UNILAC staff for their excellent assistance. This work was supported by the Access to Large Scale Facility programme under the Training and Mobility of Researchers programme of the European Union within the contract HPRI-CT-1999-00001, by the EXOTAG contract HPRI-1999-CT-50017, by the Interuniversity Attraction Poles Programme - Belgian State - Federal Office for Scientific, Technical and Cultural Affairs (IAP grant P5/07), by a Concerted Research Action (GOA/99/02, K.U. Leuven) and by the UK EPSRC. K.V.d.V. is research assistant of the FWO-Vlaanderen. A.N.A. was partially supported by the GREAT contract EPSRC GR/M79981.

References

1. K. Heyde *et al.*, Phys. Rep. **102**, 291 (1983).
2. J.L. Wood *et al.*, Phys. Rep. **215**, 101 (1992).
3. A.M. Oros *et al.*, Nucl. Phys. A **645**, 107 (1999).
4. R. Julin, K. Helariutta, M. Muikku, J. Phys. G **27**, R109 (2001).
5. A.N. Andreyev *et al.*, Nature **405**, 430 (2000).
6. M. Huyse *et al.*, Hyperfine Interact. **132**, 141 (2001).
7. N. Bijnens, PhD Thesis University of Leuven, 1998, unpublished.
8. W. Younes, J.A. Cizewski, Phys. Rev. C **55**, 1218 (1997).
9. K. Van de Vel *et al.*, Eur. Phys. J. A **17**, 167 (2003).
10. A.N. Andreyev *et al.*, Phys. Rev. C **66**, 014313 (2002).
11. K. Van de Vel *et al.*, Phys. Rev. C **68**, 054311 (2003)
12. A.N. Andreyev *et al.*, Eur. Phys. J. A **6**, 381 (1999).
13. A.N. Andreyev *et al.*, Eur. Phys. J. A **14**, 63 (2002).
14. G. Münzenberg *et al.*, Nucl. Instrum. Methods **161**, 65 (1979).
15. S. Hofmann, G. Münzenberg, Rev. Mod. Phys. **72**, 733 (2000).
16. P. Van Duppen *et al.*, Nucl. Phys. A **529**, 268 (1991).
17. A.N. Andreyev *et al.*, J. Phys. G **25**, 835 (1999).
18. J.O. Rasmussen, Phys. Rev. **113**, 1593 (1959).
19. W. Satula, R. Wyss, Phys. Scr. **T56**, 159 (1995). (1992).